Theor Chim Acta (1988) 73: 405–418

Theoretica Chimica Acta

Broken orbital symmetry and the description of valence hole states in the tetrahedral $[CrO_4]^{2-}$ anion*

R. Broer and W. C. Nieuwpoort

Department of Chemical Physics, University of Groningen, Nijenborgh 16, NL-9747 AG Groningen, The Netherlands

(Received May 11, revised October 13/Accepted October 16, 1987)

The localization of ligand-based valence holes in the tetrahedral complex ion $[CrO_4]^{2-}$ in a crystalline environment is studied by SCF calculations on the hole states, with progressively less restrictions on the spatial symmetry of the molecular orbitals. The final wavefunctions are obtained by constructing, from the symmetry broken SCF solutions, wavefunctions that exhibit again the proper transformation properties under the operations of T_d. The crystal environment of the $[CrO_4]^{2-}$ anion is represented by a point charge model. In contrast with the situation for core hole states, the projection afterwards into T_d symmetry is important. The final ionization energies, which are obtained from projected C_{3v} adapted SCF solutions, are reduced considerably ($\cong$3 eV) with respect to the T_d ΔSCF results, but the ordering of the states has not changed essentially. The calculated ionization energies compare favourably with results of XPS experiments on Na_2CrO_4. The evaluation of the energies of projected symmetry broken SCF solutions requires the calculation of hamiltonian matrix elements between determinantal wavefunctions built from mutually non-orthogonal orbital sets. An efficient method for the calculation of such matrix elements is presented.

Key words: Valence hole states — Symmetry breaking — Localized orbitals

1. Introduction

In an earlier paper [1] we discussed the localization of holes in molecular systems containing spatially equivalent sites as an example of a situation in which the

* Dedicated to Professor J. Koutecký on the occasion of his 65th birthday

relaxation of symmetry constraints on one-particle states and consequently on self-consistent fields can have drastic consequences. This "symmetry breaking" has been discussed more recently in reviews by Davidson and Borden [2] and Goscinsky [3]. These papers contain a number of important references that will not all be repeated here, but to which the reader is referred for a more thorough introduction to the subject. In [1] the case of oxygen $1s$ holes in the tetrahedral complex ion CrO_4^{2-} in a crystalline environment was treated in detail. Here we report the results of a similar investigation of a number of valence hole states. It is worth noting in advance, however, two points of difference between the description of core hole states and valence hole states.

The first point concerns the one-particle model that was introduced in [1] in order to elucidate in simple physical terms the driving forces that may lead to symmetry breaking in hole states. In this model quantum mechanical delocalization effects compete with, essentially classical, polarization effects. In the case of the $1s$ hole states the model could easily be used to predict the occurrence of hole localization and to estimate the magnitude of localization energies in various cases. This is because the $1s$ hole states are energetically so well separated from other hole states that a model involving only one state per oxygen site is quite adequate. For the valence hole states this is not so. Since the valence orbitals contain oxygen $2s$ and $2p$ as well as chromium $3d$, $4s$ and $4p$ contributions, the model would have to be extended to take these states into account. However, the large number of adjustable parameters such an extension would require renders the model less attractive.

For the sake of interest we have studied the predictions of the tetrahedral model of [1] for the case where only the oxygen $2p$ states are considered. That is, instead of one core state χ_i we now have two valence states $\chi_{\sigma i}$ and $\chi_{\pi i}$ per site (i). The two delocalization parameters (b_χ and b_π) that are needed in this case were obtained by calculating the $\sigma(2p)$ and $\pi(2p)$ hole states of the system $[O_2]^{4-}$ in a way similar to that used for the core hole states in [1]. The parameters then follow from $b_\sigma = \frac{1}{2}\{E(^2\Sigma_g^+) - E(^2\Sigma_u^+)\} \cong 1$ eV and $b_\pi = \frac{1}{2}\{E(^2\Pi_g^+) - E(^2\Pi_u^+)\} \cong$ 0.3 eV. The polarization parameter β (neglecting the difference in shape between a $2p_\sigma$ and a $2p_\pi$ hole on oxygen) was estimated in a way completely similar to that described in [1], resulting in $\beta \cong 0.6$ eV. From these data it can be concluded that even for the lowest lying valence hole states localization cannot be neglected, although its effects will be less pronounced than in the case of $1s$ hole states. More specifically, the numerical evaluation of the model predicts the lowest hole state in T_d symmetry to transform as t_2 and to consist of 90% $2p_\sigma$ orbitals i.e. $2p$ orbitals that are directed along a three-fold axis of the oxygen tetrahedron. This state is unstable with respect to symmetry lowering and the lowest states then obtained correspond essentially to the four possible $2p_\sigma$ holes on the oxygen sites, each transforming as a_1 under one of the four C_{3v} subgroups. By carrying out SCF calculations on a hypothetical system of four tetrahedrally arranged oxygen anions, $[O_4]^{8-}$, we have found these predictions to be correct. As we shall see later on, the interference of the metal orbitals leads to a quite different situation in the $CrO_4^{=}$ anion. Although localization does occur and the lowest

valence hole states are indeed found under C_{3v} symmetry, the localized hole states now correspond to the four equivalent pairs of $2p_\pi$ holes on the oxygen sites, each transforming as e under C_{3v}.

The second point of difference between valence hole states and core hole states lies in the necessity of constructing, out of the manifold of localized SCF wavefunctions obtained, wavefunctions that exhibit the proper transformation properties under the operations of T_d and then evaluating their energies. In the case of the $1s$ hole states this step could safely be left out in view of the very small magnitude of both overlap and hamiltonian matrix elements between the geometrically equivalent, but differently oriented, localized states. For the valence hole states this is no longer justified. We have therefore carried out the necessary symmetry projections, followed by the computation of the corresponding energy expectation values. Whenever the projections led to states of the same symmetry designation we have also carried out non-orthogonal configuration interaction calculations (NOCI) in order to make the final ion states mutually orthogonal as well as non-interacting. This type of calculation is not trivial, particularly when large basis sets are involved [4–9]. The methods we have employed to make these calculations practical are outlined in the appendix to this paper.

2. Self-consistent field calculations in various symmetries

The computational information (geometry, basis sets, incorporation of crystal environment) supplied in [1] also pertains to the spin-restricted SCF calculations to be reported here. The higher occupied orbital part of the ground state configuration is $\ldots 5t_2)^6\, 1e)^4\, 6a_1)^2\, 6t_2)^6\, 1t_1)^6$. Hence, in T_d symmetry, the lowest ion states are expected to be connected with these orbitals, which are predominantly composed of oxygen $2p$ orbitals. Only $5t_2$ and $1e$ contain substantial metal $3d$ contributions, 42% and 31%, respectively. The Koopmans' ionization energies (negative orbital energies) belonging to these orbitals are listed in Table 1 together with the ΔSCF results obtained from independent SCF calculations on the corresponding hole states $^2T_1$, $^2T_2$, $^2A_1$ and ^2E in T_d symmetry. The second $^2T_2$ hole state $(5t_2^{-1})$ could not be brought to convergence but its energy was estimated by assuming that the relaxation energy with respect to the Koopmans' energy of $5t_2$ is the same as that of $1e$ (0.83 eV). We see that the relative position of the levels predicted by the ground state orbital energies is preserved in the ΔSCF results. The lowest ionization energy is, however, calculated to be 7.8 eV, which differs substantially from the measured first ionization energy lying between 5 and 6 eV [10, 11]. The calulcated relaxation energies are all of the order of 1 eV as is usual for ligand-based ionizations in transition metal compounds [12]. The results obtained without the Madelung potential have been included in Table 1 to show that this potential hardly influences the relaxation behaviour. The results of hole state calculations in lower symmetries than T_d can also be found in Table 1. They are pictorially displayed in Fig. 1a. It is seen that the hole state energy is considerably lowered because of the increased relaxation freedom offered by the reduction of symmetry constraints. This effect is greater when the lower symmetry allows the hole to become maximally localized (Table 2). Thus the

Table 1. Valence hole state energies (eV) of CrO_4^{2-} with respect to the ground state

Symmetry	State	$-\varepsilon^a$	ΔSCF^a	$-\varepsilon^b$	ΔSCF^b
T_d	$^2T_2$	4.78	(3.94)[c]	12.88	(12.05)[c]
	^2E	4.21	3.37	12.37	11.54
	$^2T_2$	2.10	1.41	10.21	9.53
	$^2A_1$	2.08	0.97	10.15	9.02
	$^2T_1$	0.40	−0.33	8.55	7.83
C_{3v}	$^2A_1$		−0.58		7.50
	$^2A_2$		−1.11		7.05
	^2E		−2.11		6.04
C_{2v}	$^2A_1$		0.43		8.51 (8.69)[d]
	$^2A_2$		−0.56		7.60 (7.47)
	$^2B_1$		−1.47		6.68 (6.88)
	$^2B_2$		−1.47		6.68 (6.77)

[a] Madelung potential not included
[b] Madelung potential included
[c] Estimated (see text)
[d] Results with the real Madelung field of Na_2CrO_4 of C_{2v} symmetry

lowest hole state is found under C_{3v} symmetry. It transforms as ^2E and represents essentially the two-fold degenerate $2p_\pi$ hole that can be created on any of the oxygens. The $^2A_1$ state found in this symmetry is also well localized (Table 2) and corresponds to an oxygen $2p_\sigma$ hole. The energy of this state is higher than that of the $2p_\pi$ hole state, in contrast to what is found for the hypothetical O_4^{8-} system referred to in the Introduction. The results of ΔSCF calculations on the O_4^{8-} system are displayed in Fig. 1b. Comparing the T_d levels with those of Fig. 1a, we see that the $^2T_2$ and ^2E hole state energies for $CrO_4^{=}$ are shifted upwards with respect the $^2T_1$ state, in accordance with the metal $(3d)$-ligand $(2p)$ bonding interactions that stabilize the t_2 and e orbitals with respect to the non-bonding t_1 orbital.

To the gross atomic open shell populations of Table 2 we have added, for each case listed, the differences between the total gross atomic populations of the various hole states and those of the ground state. This is done to show that, in spite of the well-localized character of the symmetry broken hole orbitals themselves, the overall hole distribution in the final states has a much less localized appearance, because of the compensating charge shifts taking place in the closed valence shells.

3. Projection of proper symmetry states

A broken symmetry, many electron, wavefunction $|H_I, i\kappa\rangle$, transforming as the κth row of the irreducible representation i of a subgroup H_I of the molecular pointgroup G, is a member of a set of equivalent, non-orthogonal, broken symmetry functions generated from $|H_I, i\kappa\rangle$ by subjecting this function to all operations of G. By construction this set spans a representation of G which will

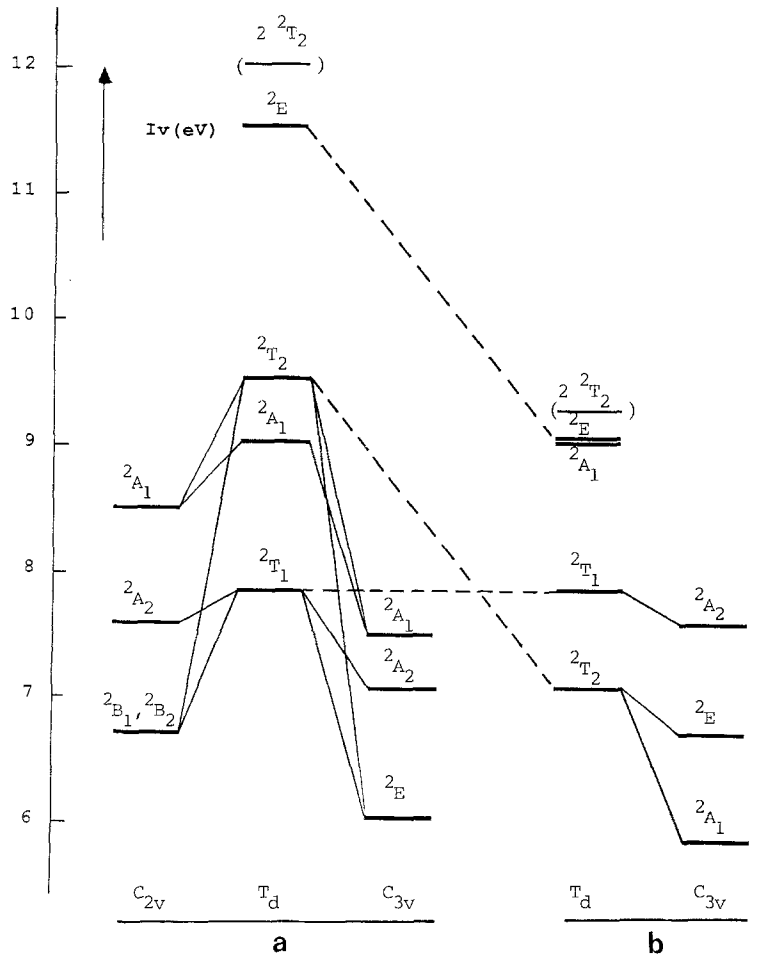

Fig. 1. **a** Valence hole state energies (I_v) of CrO_4^{2-} with respect to the ground state for T_d, C_{3v} and C_{2v} symmetries. **b** Same energies for a hypothetical O_4^{8-} system for T_d and C_{3v}. The $^2T_1$ state has been shifted to coincide with that of **a**. The very similar shifts of the $^2T_2$ and ^2E states due to bonding interactions have been indicated by *dashed lines*

in general be reducible. In the case of valence hole states, the hamiltonian matrix elements between the different members of this set cannot be neglected.

Instead of setting up the hamiltonian matrix and subsequently diagonalizing it, the irreducible components $|G, j\lambda\rangle_{i\kappa}$ of the set can be found first by means of group projection operators $O_G^{j\lambda}$

$$|G, j\lambda\rangle_{i\kappa} = O_G^{j\lambda}|H_I, i\kappa\rangle. \tag{1}$$

The corresponding energy eigenvalues can then directly be evaluated from

$$E_{Hi\kappa}^{Gj\lambda} = \frac{\langle H_I, i\kappa|HO_G^{j\lambda}|H_I, i\kappa\rangle}{\langle H_I, i\kappa|O_G^{j\lambda}|H_I, i\kappa\rangle}. \tag{2}$$

Table 2. Gross atomic populations of valence hole states of CrO_4^{2-}

Symmetry	State	Open shell populations			Difference population Q_{diff} [a]		
		Cr	O_1	O_2	Cr	O_1	O_2
T_d	^2E	1.00	0.50	0.50	−0.12	−0.22	−0.22
	$^2T_2$	0.52	1.12	1.12	−0.08	−0.23	−0.23
	$^2A_1$	0.04	0.24	0.24	−0.08	−0.23	−0.23
	$^2T_1$	—	1.25	1.25	—	−0.25	−0.25
C_{3v} [b]	$^2A_1$	0.09	0.88	0.01	−0.12	−0.28	−0.20
	$^2A_2$	—	—	0.33	+0.06	−0.19	−0.29
	^2E	0.06	2.76	0.06	−0.01	−0.39	−0.20
C_{2v} [c]	$^2A_1$	0.10	0.43	0.02	−0.08	−0.28	−0.18
	$^2A_2$	—	0.26	0.24	+0.04	−0.26	−0.26
	$^2B_1, ^2B_2$	0.02	0.48	0.01	+0.04	−0.33	−0.19

[a] $Q_{diff} = Q_{hole\ state} - Q_{ground\ state}$
[b] Equal populations on O_2, O_3 and O_4
[c] Equal populations on O_1, O_3 and on O_2, O_4

Specializing to the case at hand, we have from the C_{3v} calculations (Table 1) the sets $\{|C_{3v}, A_1\rangle\}_4$, $\{|C_{3v}, A_2\rangle\}_4$ and $\{|C_{3v}, E\rangle\}_8$ with dimensions as indicated by the lower indices outside the brackets. Their irreducible compositions under T_d are, respectively, $\{A_1, T_2\}$, $\{A_2, T_1\}$ and $\{E, T_1, T_2\}$. Basis functions of the form (1) that span these representations can be expressed in terms of two simplified group operators O^+ and O^-:

$$\begin{aligned} &|T_d, A_1\rangle_{A1} = O^+|C^1_{3v}, A_1\rangle, && |T_d, T_{21}\rangle_{A1} = O^-|C^1_{3v}, A_1\rangle \\ &|T_d, A_2\rangle_{A2} = O^+|C^1_{3v}, A_2\rangle, && |T_d, T_{11}\rangle_{A2} = O^-|C^1_{3v}, A_2\rangle \\ &|T_d, E_1\rangle_{E1} = O^+|C^1_{3v}, E_1\rangle, && T_d, T_{11}\rangle_{E2} = O^-|C^1_{3v}, E_2\rangle \\ & && |T_d, T_{21}\rangle_{E1} = O^-|C^1_{3v}, E_1\rangle \end{aligned} \tag{3}$$

where

$$\begin{aligned} &O^+ = (1 + C_{2y})(1 + C_{2z})/4, && O^{+2} = O^+ \\ &O^- = (1 - C_{2y})(1 + C_{2z})/4, && O^{-2} = O^- \end{aligned} \tag{4}$$

and C_{2y} and C_{2z} represent rotations of π around the two-fold symmetry axis y and z of Fig. 2. In (3) the subgroup C^1_{3v} has its three-fold axis in the (111) direction. The E_1 component in this subgroup is chosen to be invariant with respect to reflection in the symmetry plane defined by the z-axis and the (111) direction and the E_2 component changes sign under this operation.

For each of the degenerate T_d representations only one component is needed. These are indicated as E_1, T_{21} and T_{11} in (3) and they transform respectively as the second degree polynomial $2z^2 - x^2 - y^2$, a polar vector in the z-direction and an axial vector in the z-direction. We note that T_{21} and T_{11} both appear twice as a result of the projection of the three sets of C_{3v} solutions. Hence there remains a residual two by two interaction to be considered for each of these species.

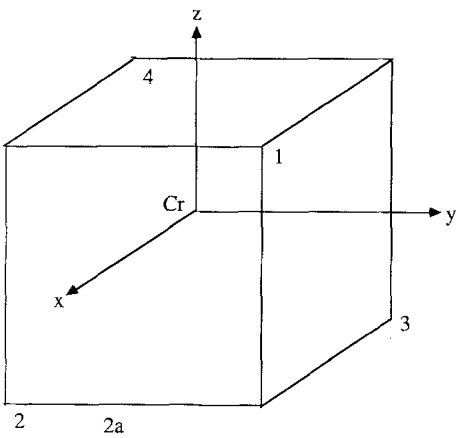

Fig. 2. Coordinate system and atomic positions a = 1.7974 bohr

4. Evaluation of the energy of projected states

The evaluation of the energy expressions (2) and the removal of the residual interactions between projected states with the same symmetry designation require the calculation of hamiltonian and metric matrix elements between determinantal wavefunctions Δ_a and Δ_b built from different, mutally non-orthogonal, molecular spin orbital sets $\{a_i\}$, $\{b_j\}$ both of dimension N (where N is the number of electrons). The matrix elements of hermitian one- and two-electron operators Ω_μ and $\Omega_{\mu\nu}$ between these determinants

$$I_1 = \langle \Delta_a | \sum_\mu \Omega_\mu | \Delta_b \rangle \tag{5}$$

$$I_2 = \langle \Delta_a | \sum_{\nu>\mu} \Omega_{\mu\nu} | \Delta_b \rangle \tag{6}$$

can be written as [13]

$$I_1 = \sum_i \sum_j \langle a_i | \Omega_1 | b_j \rangle S(i,j) \tag{7}$$

$$I_2 = \sum_{k>i} \sum_{l>j} \langle a_i a_k | \bar{\Omega}_{12} | b_j b_l \rangle S(ik, jl). \tag{8}$$

In these expressions $S(i,j)$ and $S(ik,jl)$ denote respectively the first and second order cofactors of the square matrix of overlap integrals $S_{ij} = \langle a_i | b_j \rangle$. The symbol $\bar{\Omega}_{12}$ indicates that direct and exchange contributions to the two electron interaction are included. When dealing with many electrons and large basis sets, as we do here, the calculation of I_2 by a straighforward application of Eq. (8) is hardly feasible. Firstly, the two-electron integrals must be obtained by a four index transformation on the list of integrals over basis functions. In principle this must be repeated for all different pairs of orbital sets $\{a_i\}$ and $\{b_j\}$. Secondly, the second order cofactors $S(ik,jl)$, another four index array, must be calculated

and stored. Prosser and Hagstrom [4] have shown how the calculation can be carried out efficiently. King et al. [5] recommended the use of corresponding orbitals in order to reduce the cofactor supermatrix to diagonal form. One is then left with obtaining the appropriate two-electron integral list for each matrix element. Hayes and Stone [8] and Figari and Magnasco [9] have simplified the expressions for the case that many matrix elements are needed, over many Slater determinants which differ by only a few orbitals. However the task of transforming the basic two-electron integrals remains.

This is not the case in our approach. For non-singular overlap matrices $\boldsymbol{S}$ the Jacobi theorem [14] can be used for a simple calculation of the second order cofactor super matrix (dimension N^4) from the first order cofactor matrix (dimension N^2):

$$S(ik, jl) = 2(1 - p_{ik})S(ij)S(kl)/|\boldsymbol{S}|. \tag{9}$$

Here the operator p_{ik} interchanges the indices i and k, $|\boldsymbol{S}|$ is the determinant of $\boldsymbol{S}$. Van Montfort [15] has shown that for singular matrices $\boldsymbol{S}$, the second order cofactors can also be written in a factorized form, although the two-dimensional matrices are no longer first order cofactors. Furthermore, the two electron matrix element can be written in terms of an arbitrary basis set $\{\chi\}$ which is appropriate for the expansion of the spin orbitals appearing in Δ_a and Δ_b:

$$I_2 = \sum_{p,q,r,s} \langle \chi_p \chi_r | \Omega_{12} | \chi_q \chi_s \rangle B(pr, qs) \tag{10}$$

where $B(pr, qs)$ is a transformed second order cofactor. Hence the necessary transformation is now carried out on the cofactors instead of the two-electron integrals. This yields a considerable simplification since the $B(pr, qs)$ still have a factorized form so that only two-index transformations are required. In the apendix to this paper we will prove this result in an alternative way.

5. Results

The results of the calculations of the energies of the projected C_{3v} states and of the subsequent NOCI calculations for the $^2T_1$ and $^2T_2$ states are displayed in Fig. 3. The percentage weight of the projected functions in the resolution of their respective parent states is indicated in parentheses. The T_d and C_{3v} ionization energies of Table 1 and the results of XPS [10] and X-ray emission [16] experiments on Na_2CrO_4 are included to facilitate comparisons. As expected carrying out the projections is important. The NOCI calculations are of importance only for the higher $^2T_2$ state that is shifted upward by 0.72 eV. The relevant matrix elements for this calculation are given in Table 3. The overlap between the two $^2T_1$ states is very large so that one of the new states is pushed far upwards while the other remains close to the original lower state. Although the higher-lying state represents a true upper bound for an excited $^2T_1$ state, it cannot be considered as a good approximation to it since the orbitals used are close to being optimal only for the lower state. For the $^2A_2$ state resulting from the projection of the C_{3v} $^2A_2$ states a similar statement can be made. This state is interesting since it

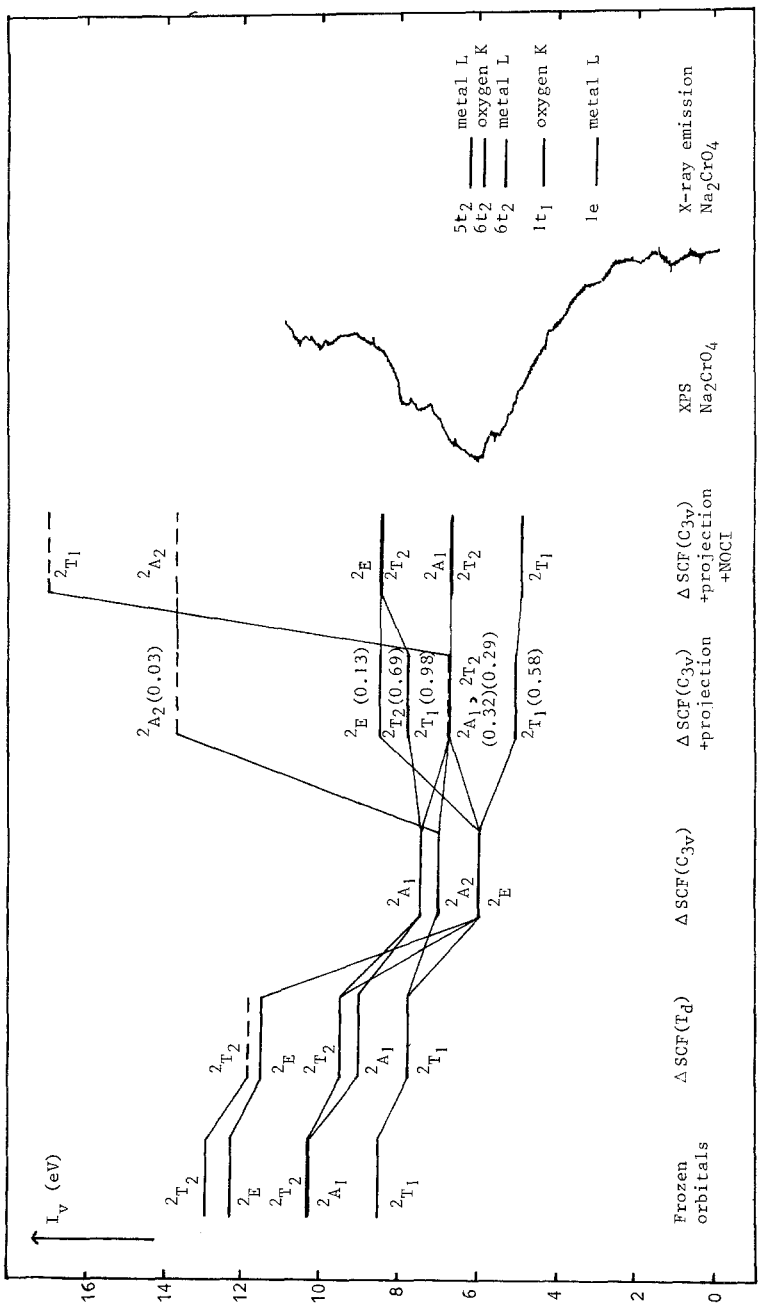

Fig. 3. Valence shell ionization energies (I_v) of CrO_4^{2-} in eV. Madelung potential included in the calculated values. Experimental data have been copied from [10]

Table 3. (a) Matrix elements between normalized wavefunctions, D, belonging to the degenerate sets $\{|C_{3v}, ik\rangle\}$

i	k	$=\langle D\|C_{2y}\|D\rangle$	$\langle D\|C_{2x}\|D\rangle$ $\langle D\|C_{2x}\|D\rangle$	$\langle D\|HC_{2x}\|D\rangle$ $=\langle D\|C_{2y}\|D\rangle$ (hartrees)	$\langle D\|HC_{2z}\|D\rangle$ (hartrees)	$\langle D\|H\|D\rangle$ +1342.0 (hartrees)
A_1		0.109738	0.109738	−147.324226	−147.324226	−0.399472
A_2		−0.299513	−0.299513	402.080895	402.080895	−0.419313
E	1	−0.064486	−0.357004	86.575458	479.296985	−0.455844
E	2	−0.259498	0.033020	348.389809	−44.331717	−0.455844

(b) Energies obtained after symmetry projection (E^{proj}) and non-orthogonal configuration interaction (E^{NOCI})

i (C_{3v})	i (T_d)	$E^{\text{proj}}+1342.0$ (hartrees)	$E^{\text{NOCI}}+1342.0$ (hartrees)	Ionization energy (eV)
A_1	A_1	−0.42704		6.78
	T_2	−0.38607	−0.36411	8.49
A_2	A_2	−0.17149		13.73
	T_1	−0.42571	−0.04645	17.13
E	E	−0.36418		8.49
	T_1	−0.49069	−0.49695	4.87
	T_2	−0.42664	−0.43112	6.66

has no counterpart in the frozen orbital or ΔSCF collection of states. It cannot be obtained by a simple orbital ionization process but requires a simultaneous excitation to configurations of the type $e)^2\, a_1^*)^1$, $e)^3\, t_2)^5\, t_2^*)^1$ or $e)^3\, t_1)^5\, t_1^*)^5$, for example.

The final ionization energies obtained are reduced considerably (3 eV) with respect to the T_d ΔSCF results, but the ordering of the states is not essentially changed.

6. Comparison with experiment

The XPS spectrum of Na_2CrO_4 has been reported by Connor et al. [10], that of Li_2CrO_4 by Prins and Novakov [11]. Since the Madelung potential used in our calculations is based upon the crystal data of Na_2CrO_4, the valence part of the spectrum of this compound is reproduced in Fig. 3. The inclusion of the potential allows an absolute comparison to be made between calculated and measured ionization energies. The overall agreement between the position of the projected, symmetry-broken, hole states and the experimental data is satisfactory. Connor et al. [10] have combined the X-ray emission data of Best [16] and Fisher [17] with their own measurements of metal and oxygen core ionization energies. Their conclusions concerning the position of the final valence hole states taking part in the X-ray emission are included in Fig. 3, together with an indication of the initial states involved. Note that the third (metal K) and fourth (oxygen K) levels actually refer to the same final state and should therefore coincide. The

fact that they do not is indicative of the error margins that should be kept in mind when comparing the emission data with the XPS results. These authors also attempted to assign the four final emission states to specific molecular orbital hole states. These assignments were based on relative intensities, calculated by means of the valence and core orbitals obtained from a small basis set SCF calculation on the ground state of the CrO_4^{2-} anion. Thus they associate the four levels in increasing order of energy with holes created in the $1e$, $1t_1$, $6t_2$ and $5t_2$ valence molecular orbitals, respectively. The assignment of ^2E to the lowest hole state, however, is inconsistent with their own calculated orbital energy pattern as well as with our results displayed in Fig. 2, as well as the results of other theoretical studies [18, 19]. In fact we see no conceivable way for the ^2E state, that appears consistently as the highest or nearly highest of the group of valence hole states, to become the lowest of these states by a more elaborate configuration interaction treatment. On the other hand, intensity calculations based on ground state orbitals may well be inadequate in this case. Generally, the relaxation of the wave function of the hole states involved in the X-ray transitions should be taken into account.

7. Concluding remarks

In this paper we have concentrated on a broken symmetry approach to the description of certain excitations and ionizations in systems with spatial symmetry. It was shown that when the energetic effects accompanying localization and delocalization respectively are of comparable magnitude, projection onto properly symmetrized final wave functions is essential. Since only a small number of non-orthogonal components usually appear, the method described to calculate the hamiltonian matrix elements makes the use of such projected functions a fairly routine matter. We note, however, that certain CI approaches based on the usual symmetrized occupied and virtual orbital spaces obtained in symmetry restricted SCF procedures may offer valuable and perhaps equally efficient alternatives. Benard et al. [20] have shown for valence hole states of transition metal dimers that energy lowerings with respect to a symmetry restricted SCF solution obtained by either relaxing the symmetry constraints or by CI based on internal single and semi-internal double excitations in the valence shell are comparable in magnitude. This type of CI has also been successfully used by Janssen and Nieuwpoort in describing crystal field and charge transfer states in solid NiO [21, 22]. The importance of translation symmetry breaking in order to obtain a good first order description of $3d$-related excitations is emphasized in earlier work on CuCl and CuBr [21, 23].

Appendix: Matrix elements between determinants based on different non-orthogonal orbital sets

Consider two determinantal N electron wave functions ($N = N^+ + N^-$):

$$\Delta_a = (N!)^{-1/2} |a_1^+ \alpha a_2^+ \alpha \cdots a_N^+ + \alpha a_1^- \beta a_2^- \beta \cdots a_N^- \beta| \tag{11}$$

$$\Delta_b = (N!)^{-1/2} |b_1^+ \alpha b_2^+ \alpha \cdots b_N^+ + \alpha b_1^- \beta b_2^- \beta \cdots b_N^- \beta|. \tag{12}$$

The superscripts $\sigma = +,-$ indicate that the spin orbitals $a_i^+\alpha$ and $a_i^-\beta$ may have different orbital parts. The orbital overlap integrals $S_{ij}^\sigma = \langle a_i^\sigma | b_j^\sigma \rangle$ may have non-zero values for all i and J. For spin independent operators Ω_1 and Ω_{12} the integrations over the spin coordinates in eqs. 7 and 8 (section 4) can be carried out beforehand, so that:

$$I_1 = \sum_i \sum_j \langle a_i^+ | \Omega_1 | b_j^+ \rangle S^+(i,j) D^- + \sum_i \sum_j \langle a_i^- | \Omega_1 | b_j^- \rangle S^-(i,j) D^+ \tag{13}$$

$$\begin{aligned} I_2 = \sum_{k>i} \sum_{l>j} \{ & \langle a_i^+ a_k^+ | \bar{\Omega}_{12} | b_j^+ b_l^+ \rangle S^+(ik,jl) D^- \\ & + \langle a_i^- a_k^- | \bar{\Omega}_{12} | b_j^- b_l^- \rangle S^-(ik,jl) D^+ \} \\ & + \sum_{i,j} \sum_{k,l} \langle a_i^+ a_k^- | \Omega_{12} | b_j^+ b_l^- \rangle S^+(i,j) S^-(k,l). \end{aligned} \tag{14}$$

Here $S^\sigma(i,j)$ and $S^\sigma(ik,jl)$ denote first and second order cofactors of the orbital overlap matrices S^σ. D^σ is the determinant of S^σ.

As an intermediate step in deriving the final equations we employ the corresponding orbitals of Amos and Hall [24]. The corresponding orbitals can be obtained by performing a unitary transformation on the orbital sets $\{a^\sigma\}$ and $\{b^\sigma\}$:

$$c_i^\sigma = \sum_j a_j^\sigma U_{ji}^\sigma \tag{15}$$

$$d_i^\sigma = \sum_j b_j^\sigma V_{ji}^\sigma \tag{16}$$

where $\boldsymbol{U}^\sigma$ and $\boldsymbol{V}^\sigma$ are the matrices that diagonalize $(\boldsymbol{S}^\sigma)(\boldsymbol{S}^\sigma)\dagger$ and $(\boldsymbol{S}^\sigma)\dagger(\boldsymbol{S}^\sigma)$, respectively. The overlap matrices between the new sets of orbitals are diagonal

$$\langle c_i^\sigma | d_j^\sigma \rangle = \lambda_i^\sigma \delta_{ij}. \tag{17}$$

Since the transformations leave the wave functions Δ_a and Δ_b unchanged, we have

$$I_1 = \sum_i \langle c_i^+ | \Omega_1 | d_i^+ \rangle \prod_{m \neq i} \lambda_m^+ \prod_n \lambda_n^- + \sum_i \langle c_i^- | \Omega_1 | d_i^- \rangle \prod_{m \neq i} \lambda_m^- \prod_n \lambda_n^+ \tag{18}$$

and

$$\begin{aligned} I_2 = & \sum_{k>i} \langle c_i^+ c_k^+ | \bar{\Omega}_{12} | d_i^+ d_k^+ \rangle \prod_{m \neq i,k} \lambda_m^+ \prod_n \lambda_n^- + \sum_{k>i} \langle c_i^- c_k^- | \bar{\Omega}_{12} | d_i^- d_k^- \rangle \prod_{m \neq i,k} \lambda_m^- \prod_n \lambda_n^+ \\ & + \sum_i \sum_k \langle c_i^+ c_k^- | \Omega_{12} | d_i^+ d_k^- \rangle \prod_{m \neq i} \lambda_m^+ \prod_{n \neq k} \lambda_n^-. \end{aligned} \tag{19}$$

These expressions are very simple to evaluate, once the integrals in terms of these corresponding orbitals are available. However, they are usually not available, since they were calculated in terms of some set of basis orbitals $\{\chi\}$ into which $\{a^\sigma\}$ and $\{b^\sigma\}$ are expanded. Using (15) and (16) the sets of corresponding orbitals can be expressed in these basic orbitals:

$$c_i^\sigma = \sum_p \chi_p C_{pi}^\sigma \tag{20}$$

$$d_i^\sigma = \sum_p \chi_p D_{pi}^\sigma. \tag{21}$$

Substitution of (20) and (21) into (18) and (19) gives for the matrix elements:

$$I_1 = \sum_{p,q} \langle \chi_p | \Omega_1 | \chi_q \rangle \{ \sum_i C_{pi}^+ D_{qi}^+ \prod_{m \neq i} \lambda_m^+ \prod_n \lambda_n^- + \sum_i C_{pi}^- D_{qi}^- \prod_{m \neq i} \lambda_m^- \prod_n \lambda_n^+ \} \tag{22}$$

$$I_2 = \sum_{p,q,r,s} \langle \chi_p \chi_r | \Omega_{12} | \chi_q \chi_s \rangle B(pr, qs) \tag{23}$$

with

$$\begin{aligned} B(pr, qs) = (1 - p_{qs}) \Big\{ & \sum_i C_{pi}^+ D_{qi}^+ \sum_{k \neq i} C_{rk}^+ D_{sk}^+ \prod_{m \neq i,k} \lambda_m^+ \prod_n \lambda_n^- \Big\} \\ & + \sum_i C_{pi}^- D_{qi}^- \sum_{k \neq i} C_{rk}^- D_{sk}^- \prod_{m \neq i,k} \lambda_m^- \prod_n \lambda_n^+ \} \\ & + \sum_i C_{pi}^+ D_{qi}^+ \sum_k C_{rk}^- D_{sk}^- \prod_{m \neq i} \lambda_m^+ \prod_{n \neq k} \lambda_n^- . \end{aligned} \tag{24}$$

Here p_{qs} interchanges the indices q and s. The four-index term $B\ (pr, qs)$, which is in fact a transformed second order cofactor, can be factorized. In order to show this we introduce the following notation:

$$X_{pq}^{\sigma} = \sum_i{}' C_{pi}^{\sigma} D_{qi}^{\sigma} (\lambda_i^{\sigma})^{-1} \tag{25}$$

$$Y_{\mu,pq}^{\sigma} = C_{p\mu}^{\sigma} D_{q\mu}^{\sigma} \tag{26}$$

$$\Delta = \prod_m{}' \lambda_m^+ \prod_n{}' \lambda_n^- . \tag{27}$$

The prime on summation and multiplications indicates that terms with $\lambda_i^{\sigma} = 0$ are excluded. The acutal form of the factorized cofactors depends on the number of zero eigenvalues of the overlap matrices. If none of the overlap eigenvalues is zero, (24) can be written as

$$B(pr, qs) = \Delta \{ (1 - p_{qs}) (X_{pq}^+ X_{rs}^+ + X_{pq}^- X_{rs}^-) + X_{pq}^+ X_{rs}^- \} \tag{28}$$

and the one electron matrix element is simply

$$I_1 = \Delta \sum_{p,q} \langle \chi_p | \Omega_1 | \chi_q \rangle (X_{pq}^+ + X_{pq}^-) . \tag{29}$$

If one of the overlap eigenvalues is zero, $\lambda_{\mu}^{\sigma} = 0$, one of the first two terms in (24) is zero and we have

$$B(pr, qs) = \Delta \{ 2(1 - p_{qs}) Y_{\mu,pq}^{\sigma} X_{rs}^{\sigma} + Y_{\mu,pq}^{\sigma} X_{rs}^{\sigma'} \}, \qquad \sigma' \neq \sigma \tag{30}$$

$$I_1 = \Delta \sum_{p,q} \langle \chi_p | \Omega_1 | \chi_q \rangle Y_{\mu,pq}^{\sigma} \tag{31}$$

In case of two zero overlap eigenvalues, two cases must be distinguished.

Firstly, if the zero eigenvalues belong to the same spin, $\lambda_{\mu}^{\sigma} = \lambda_{\nu}^{\sigma} = 0$, only one of the first two terms in (24) is nonzero, and we have

$$B(pr, qs) = \Delta (1 - p_{qs}) Y_{\mu,pq}^{\sigma} Y_{\nu,rs}^{\sigma} . \tag{32}$$

Secondly, if the zero eigenvalues belong to different spins, $\lambda_{\mu}^{\sigma} = \lambda_{\nu}^{\sigma'} = 0$ with $\sigma' \neq \sigma$, the first two terms in (24) are zero:

$$B(pr, qs) = \Delta Y_{\mu,pq}^{\sigma} Y_{\nu,rs}^{\sigma'} \tag{33}$$

An essential practical advantage of employing Eq. (23) with (28), (30), (32) or (33) is that a four index transformation is avoided and replaced by the calculation of the matrices $\boldsymbol{X}^+$ and $\boldsymbol{X}^-$, which is equivalent to performing a two index transformation. Note, that $\boldsymbol{Y}_\mu^\sigma$ is a simple matrix product of two row vectors.

The method has been implemented in a program, GNOME [25]. $\boldsymbol{U}^\sigma$ and $\boldsymbol{V}^\sigma$ are calculated using a standard single value decomposition technique. Subsequently $\boldsymbol{C}^\sigma$ and $\boldsymbol{D}^\sigma$ are evaluated, and from these the "transformed cofactors" $\boldsymbol{X}^\sigma$ are evaluated. Integrals for the calculation of the one electron matrix elements are evaluated directly in the program. In the two electron part a file of electronic repulsion integrals, generated by our SCF- and CI-package SYMOL [26], is processed sequentially. For clarity in the expressions involving summations over basis functions, no use is made of the permutation symmetry with respect to the indices p, q, r, s. In the actual program the above formulas are implemented using the unique two electron integrals only.

Recently, rather similar considerations have been presented by Petsakalis et al. [27].

References

1. Broer R, Nieuwpoort WC, (1981) Chem Phys 54:291
2. Davidson ER, Borden WT (1983) J Phys Chem 87:4783, and references therein
3. Goscinski O, (1986) Int J Quant Chem: Quant Chem Symp 19:51, and references therein
4. Prosser F, Hagstrom S (1986) Int J Quant Chem 2:89
5. King HF, Stanton RE, Wyatt HKRE, Parr RG (1967) J Chem Phys 47:1936
6. Martin RL, (1981) J Chem Phys 74:1852
7. Leasure SC, Balint-Kurti GG (1985) Phys Rev A31:2107
8. Hayes IC, Stone AJ (1984) Mol Phys 53:69
9. Figari G, Magnasco V (1985) Mol Phys 55:319
10. Connor JA, Hillier IH, Saunders VR, Wood MH, Barber M (1972) Mol Phys 24:497
11. Prins R, Novakov T (1972) Chem Phys Lett 16:86
12. Zeinstra JD, Nieuwpoort WC (1978) Inorg Chim Acta 30:103
13. Löwdin PO (1955) Phys Rev 97:1474
14. Löwdin PO (1955) Phys Rev 97:1490; Aitken AC (1959) Determinants and matrices. Oliver & Boyd, Edinburgh
15. van Montfort JTh (1980) Ph.D. Thesis, University of Groningen
16. Best PE (1966) J Chem Phys 44:3248
17. Fisher DW (1969) J Appl Phys 40:4151
18. Hillier IH, Saunders VR (1971) Chem Phys Lett 219
19. Gubanov VA, Weber J, Connolly JDW (1975) J Chem Phys 63:1455; Weber J (1976) Chem Phys Lett 40:275
20. Benard M, (1982) Theor Chim Acta 61:(1982) 61:379; Cox PA, Benard M, Veillard A (1982) Chem Phys Lett 87:159; Benard M (1983) Chem Phys Lett 96:183
21. Janssen GJM (1986) Ph.D. Thesis, University of Groningen
22. Janssen GJM, Nieuwpoort WC: submitted for publication in Phys Rev B
23. Janssen GJM, Nieuwpoort WC (1985) Phil Mag B51:127; Janssen GJM, Nieuwpoort WC (1985) Solid State Ionics 16:29
24. Amos AT, Hall GG (1961) Proc Royal Soc A 263:483
25. Broer R (1981) Ph.D. Thesis, University of Groningen
26. van der Velde GA (1974) Ph.D. Thesis, University of Groningen
27. Petsakalis LD, Theodorakopoulos G, Nicolaides CA, Buenker RJ, Peyerimhoff, SD (1984) J Chem Phys 81:3161